ISSN (Print) 1226-1750
ISSN (Online) 2233-6656
Journal of Magnetics 27(3), 298-302 (2022) https://doi.org/10.4283/JMAG.2022.27.3.298

Prediction of Conductor Ratio for Tubular Linear Induction Motors using Finite Element Method and Response Surface Methodology

Min-Ro Park[1] **and Kyu-Seob Kim**[2]*

[1]*Department of Electrical Engineering, Soonchunhyang University, Asan 31538, Republic of Korea*
[2]*Department of Automotive Engineering, Gyeongsang National University, Jinju 52725, Republic of Korea*

(Received 27 April 2022, Received in final form 8 June 2022, Accepted 29 June 2022)

In many countries, the demand for motors has rapidly increased. For equipment automation and energy reduction, motors are efficient machines and play an important role in alleviating the current energy crisis. However, rotary machines have been studied instead of linear machines. Furthermore, tubular linear induction motors (TLIMs) have been developed for use in industry, but the characteristics of these machines have not been analyzed. In this study, using the finite element methodology (FEM), a TLIM was examined using the ratio of conductor thickness and back iron. The design of experiment (DOE) and response surface methodology were used to obtain this result. The TLIM is modeled to obtain thrust force in the steady state. Furthermore, conductor and back iron thickness are efficiently assigned using the DOE. The central composite design introduced in this study is used in various DOE methods. As a result, the conductor and back iron thickness ratio is obtained at an optimum value. This ratio can be used to design the TLIM for low voltages.

Keywords : design of experiment (DOE), finite element method (FEM), equivalent magnetic circuit network method, optimization, tubular linear induction motor (TLIM), response surface methodology (RSM)

1. Introduction

In all modern industries, the demand for factory automation and energy-saving is increasing to improve productivity and reduce the unit cost of production. Particularly, motors are used as power sources in many industries. Hence, their performance and characteristics play an important role in energy reduction and automation [1]. In general, several industrial machines are rotary types, which are ineffective for systems requiring linear motion. If a rotary-type motor is used on a linear motion system, a loss of gear, ball screw, and belt due to mechanical friction is generated. Additionally, complex circuit composition and efficiency are not reasonable. Therefore, a linear motion motor was developed to generate a straight thrust force. This machine is a tubular linear induction motor (TLIM) with various applications [2].

Design of experiment (DOE) is the application of statistics to design an efficient method and analyze the results of using the method. In other words, for resolving an unfamiliar situation, the DOE entails conducting an experiment, obtaining results, and analyzing the results. Through this method, a minimum number of experiments can be conducted to obtain the necessary information. DOE advanced from agriculture in 1920, and since then, it has been applied in medical science, engineering, experimental psychology, and sociology. This study applies a central composite design along with the DOE.

Through the DOE, sampling points are obtained. Then, optimal solutions are obtained using the response surface methodology (RSM) about sampling points. The approximate polynomial equation of the system's response to a complex combination of parameters is the effect of design parameters, and the response surface has the optimal design. The DOE is an optimal combination of design parameters, and the RSM helps obtain a mathematical relationship of the combination of design parameters.

*Corresponding author: Tel: +82-55-772-3641
Fax: +82-55-772-3649, e-mail: ks.kim@gnu.ac.kr

2. Analysis Model and Design Parameter

2.1. Analysis model

In this study, the TLIM was analyzed for power values of 200, 300, 400, 500, and 600 W. The fundamental

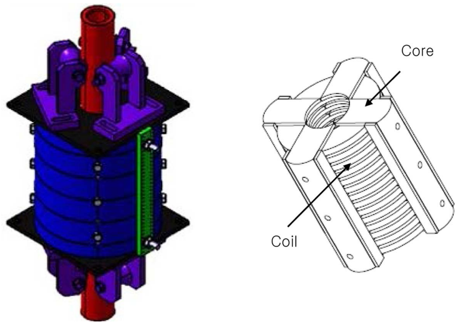

Fig. 1. (Color online) Structure of TLIM.

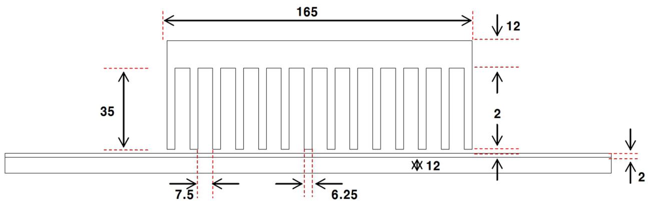

Fig. 2. (Color online) Initial model.

Table 1. Specification of the TLIM.

	Value
Number of poles	2
Number of phases	3
Number of slots	13
Input voltage	220 V
Frequency	7 Hz
Conductor conductivity	3.12×10^7 S/m
Back iron conductivity	0.5×10^7 S/m
Mover material	S23

model is given in Fig. 1. The primary of a flat linear induction motor is rolled about an axis parallel to the direction of the traveling field. The field travels along the bore of the stator (or primary). The mover consists of a cylindrical ferromagnetic core with a conducting sleeve. The main advantages of the TLIM are that it is rugged and easy to construct. The TLIM is particularly suited for short-stroke applications [3, 4].

In this study, the 2p/13s model is presented. The initial model's dimensions are shown in Fig. 2, and the specifications of the TLIM are summarized in Table 1. The TLIM introduced in this study is a two-pole machine, and the winding configuration is shown in Fig. 3 [5].

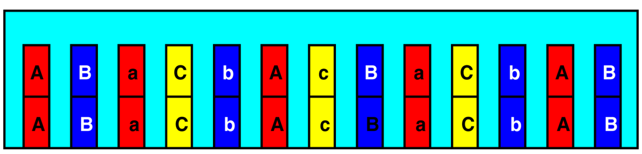

Fig. 3. (Color online) Winding configuration.

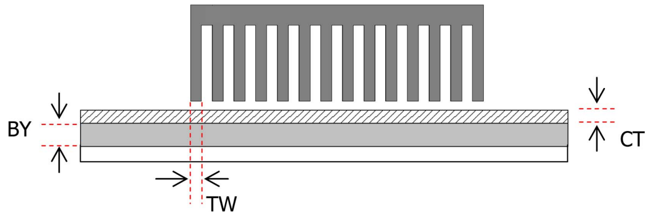

Fig. 4. (Color online) Variable for optimal design.

2.2. Design parameters

The optimal design parameters are conductor thickness, stator back iron, and tooth width. In linear motor minimum, the conductor and back iron thicknesses are required to obtain the maximum thrust force, and the tooth width can be for various shapes.

Fig. 4 shows the optimum design variables. The tooth width was determined using the equivalent magnetic circuit method and excluded from the optimal design.

3. Analysis Theory

In this section, analysis theory shows the design of minimum reluctance for the tooth width and optimum design.

3.1. Design of minimum reluctance

The tooth and yoke widths must be determined to obtain more output power. We employed an equivalent magnetic circuit comprising components that move separately to compute this width. Hence, the tooth and yoke widths are determined with minimum reluctance. The following assumptions are required in the equivalent magnetic circuit network method [4]:

1) Permeability of tooth and yoke is constant.

2) End effects are not considered.

3) HT, AL, and slot area are determined in the initial design.

4) Leakage flux is not considered.

Fig. 5 shows the equivalent magnetic circuit of the mover.

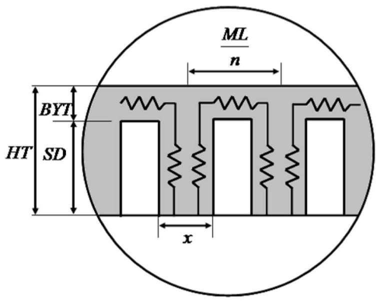

Fig. 5. Equivalent magnetic circuit of mover.

$$R_{total} = R_{tooth} + R_{yoke} = 2 \times x \cdot L_{st} / \mu\left((HT+SD)/2\right) + \left((HT-SD)\cdot L_{st} / \mu((ML/n)-x)\right) \quad (1)$$

$$SD = slot\ area / ((ML/n)-x) \quad (2)$$

where R_{total} is the total reluctance, R_{tooth} is the tooth reluctance, R_{yoke} is the yoke reluctance, L_{st} is the stack length, μ is the permeability, and x is the tooth width [6].

3.2. Optimum design

For performing the optimum design in target TLIM, DOE, and RSM are used.

In the design, DOE is applied before RSM. As the DOE is conducted, high efficiency may be obtained if various design parameters and high levels are used. However, in this case, the sampling point increases geometrically. Therefore, higher costs are incurred, and more effort is required because of limited time for high levels. To avoid this effort, DOE is needed. Results can be obtained from the DOE through efficient placement for a minimum experiment.

DOE provides the number of undetermined response shape coefficients and the supposed approximate model. When applying the 2nd order polynomial regression model, n^k factorial design (FD), central composite design, and D-optimal design are generally used.

The CCD optimal was used in this study instead of FD and D-optimal designs. To avoid the disadvantages of FD and increase efficiency, CCD uses the shape of n^k factorial design for the central and axial points. In n^k FD, the k is the number, and the lever is n. n^k FD is efficient for linear response. However, the curvature of the response value is not detected. Practical utilization is limited. Additionally, this method becomes less efficient with increasing design variables because of the increasing number of experiments [7, 8].

CCD is composed of five design variables with five levels, and it has nine sampling points for two variables. This explanation is presented in Fig. 6. This method has a higher level than the factorial design, so the surface response is efficiently presented. Equations (3) and (4) present the number of FD and CCD.

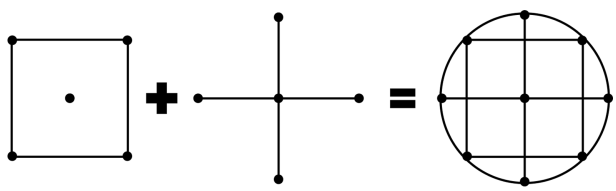

Fig. 6. Design of experiment-CCD.

$$NS_{FD} = n^k \quad (3)$$

$$NS_{CCD} = 2^k + 2k + n_c \quad (4)$$

where n_c is the number of central points greater than one. If the number of design variables is three, the sampling point of 3k factorial design is 27, but CCD is 15, indicating that CCD is more efficient than FD.

The experiment is conducted by sampling the points of obtaining DOE. This result is applied to RSM. RSM is the method that is a function of the relation between the design variables and response. Through the result of DOE, first-order and second-order least square regression approximations are conducted. Moreover, to analyze the accuracy of the regression curve, the R^2 and adjusted R^2 are used. This coefficient is the error between the exact value and estimation of the regression curve [9].

R^2 and adjusted R^2 are calculated as follows:

$$R^2 = \frac{SSR}{SST} \quad (5)$$

$$adjust\ R^2 = 1 - \frac{SSR/(N-k)}{SST/(N-1)} \quad (6)$$

where N is the total number of experiments, and k is the number of design variables. SST, SSR, and SSE are calculated as follows:

$$SST = \sum_{u=1}^{N} (y_u - \bar{y})^2 \quad (7)$$

$$SSR = \sum_{u=1}^{N} (\hat{y}_u - \bar{y})^2 \quad (8)$$

$$SSE = \sum_{u=1}^{N} (y_u - \hat{y})^2 \quad (9)$$

where y is the actual response, $\bar{y}$ is the mean value of the actual response, and $\hat{y}$ is the regression estimation [10]. R^2 and the adjusted R^2 are between 0 and 1, and values closer to 1 represent a good approximation.

4. Result and Discussion

According to each output power, the regression curve is given by the following equations:

$$Y_{200W} = 2.5414 - 3.8624A + 1.6871B - 3.6687C - 7.1468A^2 - 0.4254B^2 + 0.5106C^2 + 0.2200AB + 4.8900AC + 0.0775BC \quad (10)$$

$$Y_{300W} = -127.069 + 13.5182A + 30.4581B + 20.1841C - 3.8086A^2 - 5.0940B^2 - 1.3332C^2 + 3.0133AB - 0.8644AC + 0.5111BC \quad (11)$$

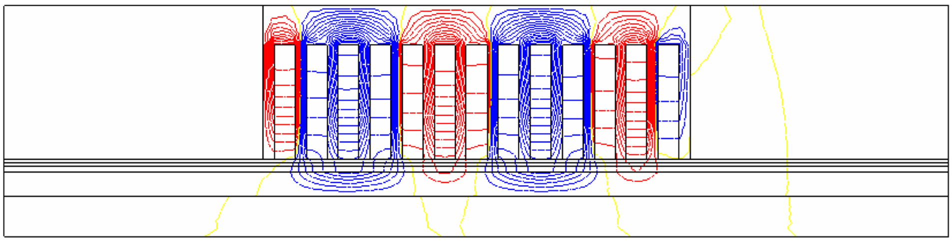

Fig. 7. (Color online) Equi-potentials of 400 W at the rated condition (slip:0.5).

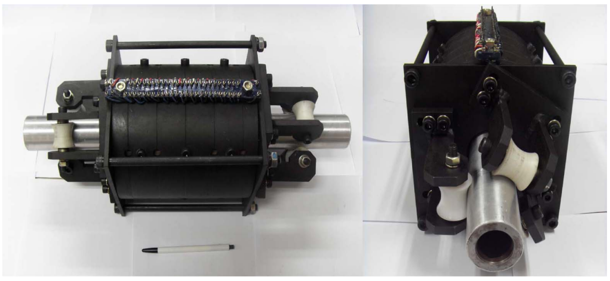

Fig. 8. (Color online) Fabricated TLIM.

$$Y_{400W} = -5.03185 - 26.0310A + 15.8675B + 7.4655C - 4.6410A^2 - 0.7713B^2 - 0.5547C^2 + 0.3987AB + 4.5381AC + -0.9943BC \quad (12)$$

$$Y_{500W} = 20.2838 + 13.0798A - 0.6742B - 1.7004C - 0.5972A^2 + 2.5446B^2 + 0.6460C^2 - 4.0296AB - 4.0296AC - 1.8988BC \quad (13)$$

$$Y_{600W} = 27.3360 + -0.9205A + 23.9074B - 12.4568C + 1.4271A^2 - 1.3070B^2 + 0.6125C^2 + 0.0817AB + 0.0819AC - 0.5197BC \quad (14)$$

where A is CT, B is TW, and C is BY. R^2 and the adjusted R^2 are 0.89 and 0.80, respectively, @400 W, which is somewhat low.

Fig. 7 shows the equipotential distribution of TLIM under the rated condition of 400 W, and Fig. 8 shows the fabricated TLIM.

Fig. 9 shows the optimum design of 400 W. This response surface shows the three design variables that are various combinations of DOE. These three graphs show the maximum thrust force response surface. The optimum design of each power obtained with the RMS is summarized in Table 2.

Table 2. Result of the optimum design.

	A (mm)	B (mm)	C (mm)
200W	0.83	3.32	6.68
300W	1.50	3.75	7.79
400W	3.68	3.31	13.36
500W	4.60	4.14	16.70
600W	5.52	7.5	15.00

The output power and the ratio of the conductor thickness and back iron converges to 2.8. If the conductor thickness is constant, the power capacity increases, and

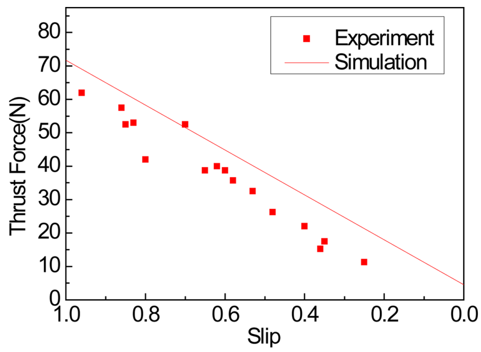

Fig. 10. (Color online) Comparison of thrust force according to slip.

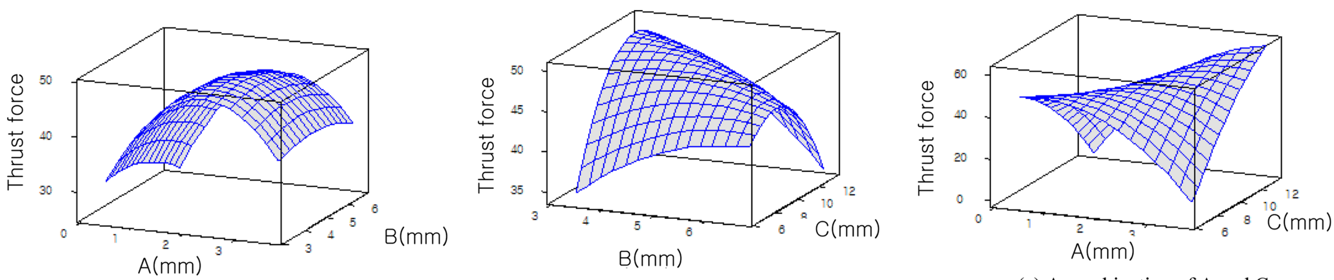

(a) A combination of A and B (b) A combination of B and C (c) A combination of A and C

Fig. 9. (Color online) Response surface model @ 400 W.

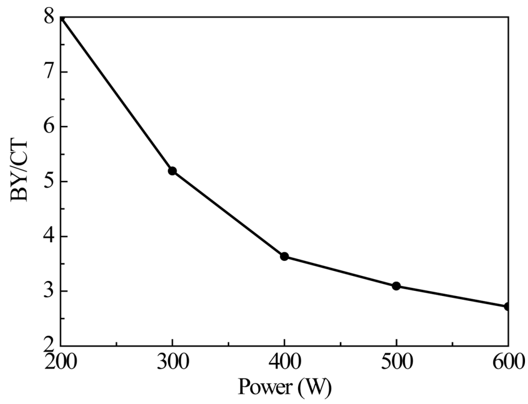

Fig. 11. Ratio of BY to CT according to power.

the back iron thickness decreases.

Fig. 10 shows the thrust force comparison of the experiment and simulation. Measurements conducted with DC power supply agree with the experiments.

Fig. 11 shows this result. This result is why TLIM should perform a certain standard thrust force in a limited voltage.

5. Conclusion

In this study, optimum TLIM designs are obtained using DOE and RSM. To examine the ratio of BY and CT according to power based on the typical TLIM capacity, we minimized the reluctance of the back yoke. This minimization was used to determine the optimal shape of the TLIM and analyze the thrust according to slip. Finally, the ratio of BY and CT of TLIMs according to power is examined in this study. The result shows that for large powers, the ratio of BY and CT converges to 2.8. Although this result is for a constant voltage, the ratio is helpful to the design of TLIMs, which are low voltage devices.

References

[1] I. Boldea and S. A. Nasar, Linear Motion Electromagnetic Systems, John Wiley & Sons (1985).
[2] T. A. Lipo, Introduction to AC Machine Design Vol. 1, WISCONSIN power electronics research center university of WISCONSIN (1996).
[3] R. Haghmaram and A. Shoulaie, IEEE Trans. Magn. **42**, 1687 (2006).
[4] B. H. Lee, K. S. Kim, S. O. Kwon, T. Sun, J. P. Hong, and J. H. Lee, J. Magn. **16**, 3657 (2011).
[5] T. Mishima, M. Hiraoka, and T. Nomura, IEEE International Conference on Electric Machines and Drives (2005).
[6] J. Y. Lee, J. H. Chang, D. H. Kang, S. I. Kim, and J. P. Hong, IEEE Trans. Magn. **43**, 1817 (2007).
[7] X. K. Gao, T. S. Low, Z. J. Liu, and S. X. Chen, IEEE Trans. Magn. **38**, 1141 (2002).
[8] S. I. Kim, J. P. Hong, Y. K. Kim, H. Nam, and H. I. Cho, IEEE Trans. Magn. **42**, 1219 (2006).
[9] Bazghaleh, Naghashan and Meshkatoddini, IEEE Trans. Magn. **46**, 3939 (2010).
[10] K. Baoquan, L. Liyi, and Z. Chengming, IEEE Trans. Magn. **45**, 250 (2009).